High-flux and high-resolution spectroscopic facility in the VUV region at Super-ACO

K. Ito,[a]* B. Lagarde,[b] F. Polack,[b] C. Alcaraz[b] and L. Nahon[b,c]

[a]*Photon Factory, Institute of Materials Structure Science, High Energy Accelerator Research Organization, Tsukuba 305, Japan,* [b]*LURE, Bâtiment 209D, Université Paris-Sud, 91405 Orsay CEDEX, France, and* [c]*CEA/DRECAM/SPAM, Bâtiment 522, CE Saclay, 91191 Gif-sur-Yvette CEDEX, France. E-mail: kenji.ito@kek.jp*

A new spectroscopic facility, consisting of a planar/helical undulator and a 6.65 m off-plane Eagle monochromator, has been designed. It can supply high-flux and high-resolution photons with 'exotic' polarization in the 5–40 eV energy range. The astigmatism can be compromised by horizontally focusing the incident radiation on the grating. The rotation of a post-focusing toroidal mirror compensates for the deviation of the exit beam caused by the grating translation. The whole system will be installed at beamline SU5 of SUPER-ACO (0.8 GeV) at the beginning of 1998. With a 4300 grooves mm^{-1} grating, a resolving power of around 10^5 is expected at 20 eV.

1. Introduction

An undulator-based high-resolution spectroscopic facility will be installed at beamline SU5 of Super-ACO in LURE. This facility is optimized for the photon energy region 5–40 eV, and aims to cover the research fields of photon-induced dynamics on cold molecules, metallic and molecular clusters, free radicals and laser-excited species.

The undulator-based Chemical Dynamics Beamline in operation at the Advanced Light Source (Koike *et al.*, 1994; Heimann *et al.*, 1996) is producing fruitful results. SU5 has a remarkable specificity due to the exotic polarization capabilities of the newly designed undulator (Nahon, Corlier *et al.*, 1997), which can generate any rotatable linear, elliptical or circular polarization. The variety in polarization affords new developments in linear- and circular-dichroism experiments on anisotropic systems, such as laser-aligned species, molecules adsorbed on surfaces, chiral molecules or magnetic materials.

In this report, we present the design concept of the SU5 optics, emphasizing the criteria for selecting a monochromator for the SU5. The characteristics of the whole system and the expected performance, such as the photon-flux distribution and the resolving power based on ray-tracing simulation, have been reported (Nahon, Lagarde *et al.*, 1997).

2. Basic concept for optical design

The utilization of undulator radiation will supply (i) a relatively high photon flux, and (ii) a small spot size at the sample level. To meet the requirements mentioned above, it is necessary to have a high resolving power of $\lambda/\Delta\lambda > 10^5$ in the photon energy range 5–40 eV. We chose to adopt an off-plane Eagle-type spectrometer because its high-resolution capability with a synchrotron radiation light source has already been proven at the Photon Factory (Ito *et al.*, 1986, 1989), at SURF II (Brown & Ginter, 1984; Morgan *et al.*, 1994) and at the Advanced Light Source (Koike *et al.*, 1994; Heimann *et al.*, 1996).

A spherical-grating monochromator (SGM) with grazing incidence was proposed instead of a normal-incidence monochromator (NIM) for the energy region of interest in this report (van Elp *et al.*, 1996; van Elp, 1997). A comparison of the performance of SGMs and NIMs is not straightforward. However, provided that the sizes of the SGM and the NIM are nearly equal, it has been shown that an SGM can provide a higher flux than an NIM. The slit widths for the SGM will be almost twice those of the NIM in cases when the resolution is determined by the slit width. The figure-slope error of the grating surface affects the resolution in a relationship proportional to the cosine of the diffraction angle. This means that the figure-slope-error effect is less in grazing-incidence mountings. The microroughness of the grating surface causes scattered light, and is more serious in the normal-incidence case. However, modern polishing technology can provide a microroughness of <0.5 nm r.m.s., and in practice the scattered light is negligible even for NIMs. The problem with the SGM is that the resolution is limited by the coma aberration, although this is diminished at a certain wavelength. The SGM designed by van Elp (1997) aims at a resolving power of $\sim 1 \times 10^4$, which does not meet our requirements. If a grazing-incidence mounting is to be used, the coma aberration should be suppressed in the wide wavelength region. This can be achieved by adopting the Rowland mounting; however, this would require much design study. In the end, we decided to choose a normal-incidence mounting to achieve high resolution for the SU5.

Various types of NIM have been developed. As mentioned above, the Rowland mounting is necessary for achieving high resolution. However, most NIMs installed at synchrotron radiation facilities are off-Rowland types (Saile, 1978; Ito *et al.*, 1995), in which the defocus term is kept at zero in the wavelength scanning. The coma aberration in the NIM is not as serious as that in a grazing-incidence monochromator; however, it is important over large rotation angles of the grating. The entrance and exit slits should be fixed during the wavelength scanning, because a storage ring and experimental apparatus are not easily moved. The deviation over the wavelength range of the emerging beam from the monochromator should be minimized for the same reason. As pointed out by Namioka (1959), the off-plane Eagle-type mounting is the only possible candidate that satisfies the present requirements. In the off-plane Eagle mounting, the entrance and exit slits are placed symmetrically above and below the Rowland circle, while the grating is rotated and translated during the wavelength scanning so that both the slits and the grating remain on the Rowland cylinder. The in-plane Eagle-mounting and other Rowland-mounting NIMs cannot be adopted for the SU5. The exit slit is forced to move in the former, and the emerging beam is deviated in the latter.

3. Beamline optics

The overall optical layout is displayed in Fig. 1. The undulator radiation travels to the entrance slit S_1 of the monochromator, installed in the centre of the Super-ACO storage ring, *via* two

toroidal mirrors, M_1 and M_2. The role of M_1 is to deflect the beam by a 2° angle in the vertical plane in order to avoid a crossing of the beamline pipe and the vacuum chamber of the ring, and to focus the beam through a gas filter made of a series of thin capillaries (minimum diameter of 2 mm) separated by two differential pumping stages. After the gas filter, the diverging beam impinges onto the grazing-incidence mirror M_2 which deflects the beam in both planes (particularly the vertical plane), so that downstream of M_2 the beamline lies in the horizontal plane. M_2 also focuses the beam vertically onto S_1. The 0.3 m distance between M_2 and S_1 leads to a demagnification of ~14, which is important in order to spread the beam footprint over a large vertical dimension so that many horizontal grating grooves are illuminated (in this case typically more than 400 000) ensuring a non-diffraction-limited resolving power.

In addition to vertical focusing, the M_2 mirror also has the role of horizontal focusing onto the grating. The advantage of this system is that the astigmatism introduced by the scanning of the gratings is negligible, without the use of a cumbersome bending system for either the pre-focusing or the post-focusing mirror. This absence of induced-astigmatism compensation leads to a small beam spot at the experimental point, with a shape and area independent of the wavelength and with a typical 500 μm (H) × 100 μm (V) size.

The undulator radiation is dispersed by switchable spherical holographic gratings with 6.65 m radii. Two gratings, G_1 (2400 grooves mm^{-1}) and G_2 (4300 grooves mm^{-1}), cover the wavelength region 30–250 nm. Note that the grating has to be translated on the bisector line of the angle formed by S_1, S_2 and the zero position of the grating during the rotation for the wavelength scanning. The grating thus stays on the Rowland cylinder. The maximum translation range is 300 mm with a 17° corresponding angle of rotation. The displacement of both slits
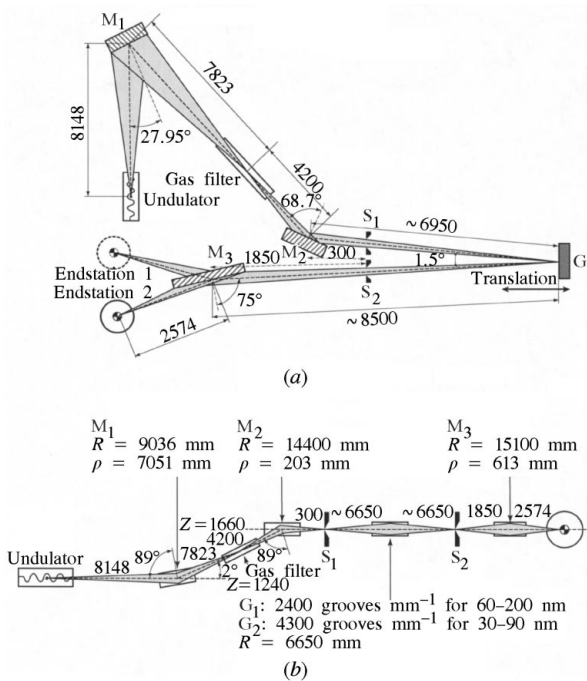

Figure 1
Optical layout of the low-energy high-resolution SU5 beamline: (*a*) top view; (*b*) side view. M_1, M_2, pre-focusing toroidal mirrors; S_1, entrance slit; S_2, exit slit; G, grating; M_3, post-focusing toroidal mirror.
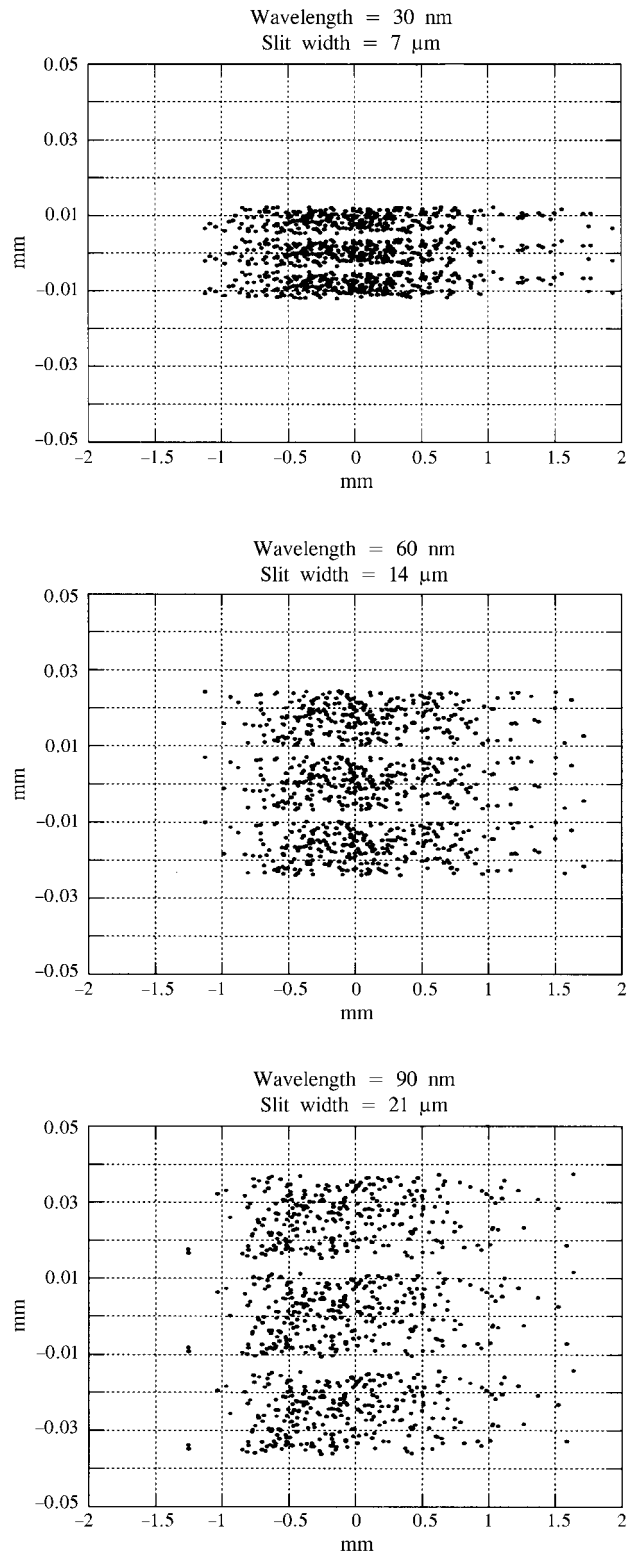

Figure 2
Ray-tracing simulations showing the beam spot size and profile in the exit-slit plane for the 4300 grooves mm^{-1} grating for λ and λ±Δλ, with λ/Δλ = 10^5, at λ = 30, 60 and 90 nm. The beam size of the light-source is assumed to be 0.39 and 0.425 mm in the horizontal and vertical directions, respectively. The photon beam divergence is taken as 0.3 mrad in both directions. The corresponding beam profiles have been rotated respectively by 0.30, 0.195 and 0.097° (see text and Namioka, 1959). This shows that the target resolving power of 10^5 can be achieved at λ = 30, 60 and 90 nm with 7, 14 and 21 μm slits, respectively.

from the Rowland plane should be minimized in order to achieve a high resolution, and is 87 mm in the present case.

Fig. 2 shows the ray-tracing simulations giving the beam spot size and profile on the exit-slit plane for the G_2 grating for λ and $\lambda \pm \Delta\lambda$, with $\lambda/\Delta\lambda = 10^5$, at $\lambda = 30$, 60 and 90 nm. The beam size of the light source used in the simulation is 0.39 and 0.425 mm in the horizontal and vertical directions, respectively. The beam divergence is 0.2 mrad in both directions. This shows that the target resolving power of $\sim 10^5$ can theoretically be achieved at $\lambda = 30$, 60 and 90 nm with slits of 7, 14 and 21 μm, respectively. The entrance slit should be rotated by a small angle from the position parallel to the grating grooves (Namioka, 1959). The rectangular shape of the beam profile at any wavelength shows that the aberrations due to the grating focusing are negligible. This is an important feature of the Eagle off-plane mounting: the resolution is slit-width limited.

Finally, the monochromated beam is focused and directed towards one of the two end-stations by a post-focusing toroidal mirror, M_3. The beam spot moves by about 2 mm in the experimental point during a scan over the whole range of the gratings. This displacement is compensated for by rotation of M_3.

The total photon flux, estimated from the characteristic of the undulator radiation, the reflectivity of optical elements and the grating diffraction efficiency (calculated by scalar theory), is $>10^{10}$ photons s^{-1} with a 0.002% bandwidth in the energy region 5–25 eV. A maximum flux of $\sim 10^{11}$ photons s^{-1} is expected around 10 eV.

The whole system should be installed at the beginning of 1998, and should be available for users as a VUV high-resolution/high-flux/exotic-polarization facility in summer 1998.

References

Brown, C. & Ginter, M. (1984). *Appl. Opt.* **23**, 4034–4039.
Elp, J. van (1997). *Nucl. Instrum. Methods A*, **390**, 403–408.
Elp, J. van, Theil, C., Folkmann, F., Baurichter, A., Mythen, C. S. & Jensen, B. N. (1996). *Nucl. Instrum. Methods A*, **381**, 548–553.
Heimann, P. A., Koike, M., Hsu, C. W., Evans, M., Ng, C. Y., Blanck, D., Yang, X. M., Flaim, C., Suits, A. & Lee, Y. T. (1996). *Proc. SPIE*, **2856**, 90–99.
Ito, K., Maeda, K., Morioka, Y. & Namioka, T. (1989). *Appl. Opt.* **28**, 1813–1817.
Ito, K., Morioka, Y., Ukai, M., Kouchi, N., Hatano, Y. & Hayaishi, T. (1995). *Rev. Sci. Instrum.* **66**, 2119–2121.
Ito, K., Namioka, T., Morioka, Y., Sasaki, T., Noda, H., Goto, K., Katayama, T. & Koike, M. (1986). *Appl. Opt.* **25**, 837–847.
Koike, M., Heimann, P. A., Kung, A. H., Namioka, T., DiGennaro, G., Gee, B. & Yu, N. (1994). *Nucl. Instrum. Methods A,* **347**, 282–286.
Morgan, H., Fortna, J., Seyoum, H., Furst, M. L., Hughey, L. R., Humm, D. C. & Asfaw, A. (1994). *Nucl. Instrum. Methods A,* **347**, 287–290.
Nahon, L., Corlier, M., Peaupardin, P., Marteau, F., Marcouillé, O., Brunelle, P., Alcaraz, C. & Thiry, P. (1997). *Nucl. Instrum. Methods A,* **396**, 237–250.
Nahon, L., Lagarde, B., Polack, F., Alcaraz, C., Dutuit, O., Vervloet, M. & Ito, K. (1997). *Nucl. Instrum. Methods A,* **404**, 418–429.
Namioka, T. (1959). *J. Opt. Soc. Am.* **49**, 961–965.
Onuki, H. (1986). *Nucl. Instrum. Methods A,* **246**, 94–98.
Saile, V. (1978). *Nucl. Instrum. Methods,* **152**, 59–67.